

Synthesis of Titania-Pillared Hydrogen Tetratitanate Nanocomposites and Control of Slit Width

Masaru Yanagisawa,* Satoshi Uchida, Shu Yin, and Tsugio Sato

Institute for Chemical Reaction Science, Tohoku University, 2-1-1, Katahira, Aoba-ku, Sendai 980-8577, Japan

Received April 24, 2000. Revised Manuscript Received September 8, 2000

Slit-width-controlled $\text{H}_2\text{Ti}_4\text{O}_9/\text{TiO}_2$ nanocomposites were fabricated by stirring with $(\text{C}_n\text{H}_{2n+1}\text{NH}_3)_2\text{Ti}_4\text{O}_9$ and a titanyl acylate complex at 20 °C for 48 h followed by UV light irradiation from a 450 W high-pressure mercury lamp. $(\text{C}_n\text{H}_{2n+1}\text{NH}_3)_2\text{Ti}_4\text{O}_9$ was synthesized by an intercalation reaction with $\text{H}_2\text{Ti}_4\text{O}_9$ and $\text{C}_n\text{H}_{2n+1}\text{NH}_2$ in aqueous or heptane solution for 48 h. The remaining $\text{C}_n\text{H}_{2n+1}\text{NH}_2$ and acylate after titania incorporation was completely decomposed into CO_2 , H_2O , and NH_3 by UV light irradiation. A slit in the obtained nanocomposites was produced, and its width could be controlled by changing the carbon length of $\text{C}_n\text{H}_{2n+1}\text{NH}_2$. Furthermore, the slit expansion and the transformation of the layer structure to fiberlike TiO_2 were successfully confirmed by scanning electron microscopy photographs for the first time.

Introduction

Intercalation is a unique method for fabricating new functional materials because controlled interlayer space and beneficial systems for various purposes such as catalysis can be produced and designed easily by choosing the host and guest materials.^{1–8} To use them for catalysts, a beneficial morphology is needed.^{9,10} Owing to Pinnavaia^{11–13} and other researchers,^{1–8,39–41} pore-size-controlled silicates such as zeolites, MO_x , and $\text{MO}_x\text{--SiO}_2$ incorporated silicate (M = metal) can easily be obtained and applied for various catalytic processes.

It is known that silicate does not show a useful photocatalytic activity at all compared to semiconductors because silica itself cannot act as a charge carrier.^{14–22} Numerous attempts to make other semiconductor pillars into layered semiconductor hosts to

construct high-performance photocatalyst systems have been made by the Arakawa and Domen^{15–17} and Sato groups.^{18–22} For instance, CdS--ZnS , Fe_2O_3 , and TiO_2 incorporated $\text{H}_2\text{Ti}_4\text{O}_9$ and $\text{H}_4\text{Nb}_6\text{O}_{17}$ nanocomposites were synthesized and photocatalytic activity was enhanced by a semiconductor pillar.^{18–22} These nanocomposites are assumed to have a slit (approximately 0.5 nm) which comes from the layer structure of the host materials. However, the morphology and/or control of the slit width of nanocomposites made from the semiconductor were not investigated clearly in previous studies. In this study, the synthesis of TiO_2 -pillared $\text{H}_2\text{Ti}_4\text{O}_9$ nanocomposites and the control of their slit width by selecting different lengths of *n*-alkylamine (denoted as $\text{C}_n\text{H}_{2n+1}\text{NH}_2$) were examined. X-ray diffraction and N_2 adsorption analysis of them and direct observation of the slit were also performed.

Experimental Section

Intercalation of *n*-Alkylamine into the Interlayer of $\text{H}_2\text{Ti}_4\text{O}_9$. The host layer compound, $\text{K}_2\text{Ti}_4\text{O}_9$ powder, was prepared by calcination of a mixture of K_2CO_3 and TiO_2 at 1150 °C for 5 h.^{18–25} The hydrogen tetratitanate, $\text{H}_2\text{Ti}_4\text{O}_9$, was prepared by ion exchange reaction of $\text{K}_2\text{Ti}_4\text{O}_9$ in 1 M HCl at 60 °C for 1.5 h to improve the reactivity of the ion exchange. $\text{C}_n\text{H}_{2n+1}\text{NH}_2$ was incorporated inside the layer of $\text{H}_2\text{Ti}_4\text{O}_9$ as follows. In the case of $n = 3$, 12 mol dm^{-3} of $\text{C}_3\text{H}_7\text{NH}_2$ aqueous

* Corresponding author: Institute for Chemical Reaction Science, Tohoku University, Sendai 980-8577, Japan. Tel: +81-22-217-5597. Fax: +81-22-217-5599. E-mail: yanagi@kuroppe.icrs.tohoku.ac.jp.

- (1) Enea, O.; Bard, A. J. *J. Phys. Chem.* **1986**, *90*, 301.
- (2) Miyoshi, H.; Yoneyama, H. *J. Chem. Soc., Faraday Trans. 1* **1989**, *85*, 1873.
- (3) Torii, K. et al. *Stud. Surf. Sci. Catal.* **1991**, *60*, 81.
- (4) Kooli, F.; Sasaki, T.; Watanabe, M. *Langmuir* **1999**, *15*, 1090.
- (5) Brindley, G. W.; Sempels, R. E. *Clay Miner.* **1977**, *12*, 229.
- (6) Bovey, J.; Jones, W. *J. Mater. Chem.* **1995**, *5*, 2027.
- (7) Ohtsuka, K.; Hayashi, Y.; Suda, M. *Chem. Mater.* **1993**, *5*, 1823.
- (8) Yoneyama, H.; Haga, S.; Yamanaka, S. *J. Phys. Chem.* **1989**, *93*, 4833.
- (9) Conn, E. E.; Stumpf, P. K.; Bruening, G.; Doi, R. H. *Outlines of Biochemistry*, 5th ed.; Wiley: New York, 1987.
- (10) Atkins, P. W. *Physical Chemistry*, 4th ed.; Freeman: New York, 1990.
- (11) Pinnavaia, T. J. *Science* **1983**, *220*, 365.
- (12) Tanev, P. T.; Pinnavaia, T. J. *Science* **1995**, *267*, 865.
- (13) Tanev, P. T.; Pinnavaia, T. J. *Chem. Mater.* **1996**, *8*, 2068.
- (14) Sayama, K.; Arakawa, H.; Domen, K. *Catal. Today* **1996**, *28*, 175.
- (15) Takata, T.; Furumi, Y.; Shinohara, K.; Tanaka, A.; Hara, M.; Kondo, J. N.; Domen, K. *Chem. Mater.* **1997**, *9*, 1063.
- (16) Takata, T.; Shinohara, K.; Tanaka, A.; Hara, M.; Kondo, J. N.; Domen, K. *J. Photochem. Photobiol., A* **1997**, *106*, 145.
- (17) Ebina, Y.; Tanaka, A.; Kondo, J. N.; Domen, K. *Chem. Mater.* **1996**, *8*, 2534.

- (18) Sato, T.; Masaki, K.; Sato, K.; Fujishiro, Y.; Okuwaki, A. *J. Chem. Technol. Biotechnol.* **1996**, *67*, 339.
- (19) Sato, T.; Sato, K.; Fujishiro, Y.; Yoshioka, T.; Okuwaki, A. *J. Chem. Technol. Biotechnol.* **1996**, *67*, 345.
- (20) Sato, T.; Masaki, K.; Yoshioka, T.; Okuwaki, A. *J. Phys. Technol., Biotechnol.* **1993**, *58*, 315.
- (21) Sato, T.; Yamamoto, Y.; Fujishiro, Y.; Uchida, S. *J. Phys. Soc., Faraday Trans.* **1996**, *92*, 5089.
- (22) Uchida, S.; Yamamoto, Y.; Fujishiro, Y.; Watanabe, A.; Ito, O.; Sato, T. *J. Phys. Soc., Faraday Trans.* **1997**, *93*, 3229.
- (23) Dion, M. et al. *J. Inorg. Nucl. Chem.* **1978**, *40*, 917.
- (24) Marchand, R. et al. *Rev. Chim. Miner.* **1984**, *21*, 476.
- (25) Sasaki, T. et al. *Inorg. Chem.* **1985**, *24*, 2265.

solution was used for incorporation with $H_2Ti_4O_9$ by stirring at 50 °C for 2 days.^{21–22} In the case of $n = 8^{15–17}$ and 12, $C_nH_{2n+1}NH_2$ was incorporated as a 10 mol dm^{-3} heptane solution at reflux condition for 2 days. Stearylamine ($n = 18$) was used as a 2.5 mol dm^{-3} heptane solution at reflux condition for 2 days. Here, samples obtained after $C_nH_{2n+1}NH_2$ incorporation are designated as C- n .

Synthesis of Titania-Pillared $H_2Ti_4O_9$ Using a Titanil Acylate Complex. The titania pillar was constructed by stepwise incorporation as follows. Titanil acylate complex, $[Ti(OH)_x(CH_3COO)_y]^{z+}$, was prepared by modified methods of other researchers^{26–30,43} starting with host (C- n) powder, titanium isopropoxide, acetic acid, and water in a 1:20:400:2000 molar ratio. Host powders, C- n , were added to a clear solution of $[Ti(OH)_x(CH_3COO)_y]^{z+}$ and then stirred at 20 °C for 48 h to allow intercalation of $[Ti(OH)_x(CH_3CO_2)_y]^{z+}$. The obtained sample, $[Ti(OH)_x(CH_3COO)_y]_zTi_4O_9(C-n)$, after being filtered off and washed with water, was dispersed in water and irradiated with UV light from a 450 W high-pressure mercury lamp at 30 °C for 12 h in order to decompose organic species in the interlayer.^{21–22} The resulting materials before and after UV light irradiation are designated as $[Ti(OH)_x(CH_3COO)_y]_zTi_4O_9(C-n)$ and $H_2Ti_4O_9/TiO_2(C-n)$, respectively.

Analysis. The crystalline phases of the products were identified by X-ray diffraction analysis (XRD) (Shimadzu XD-D1) using graphite-monochromated $Cu K\alpha$ radiation. The interlayer distance was determined by the following equation:^{22–25}

$$\text{Interlayer distance} = d(200) \times \sin 104^\circ - 0.56 \text{ nm}$$

The ion exchange ratios from H^+ into $C_nH_{2n+1}NH_3^+$ of the products were determined by weight loss measured by TG-DTA analysis (RIGAKU-DENKI, TAS-200). Isotherms of N_2 adsorption and specific surface area were determined by using Shimadzu ASAP 2010. The microstructure of the products was observed by scanning electron microscopy (SEM) with 300 kV.

Results

XRD patterns of the samples after $C_nH_{2n+1}NH_2$ incorporation (C- n) are shown in Figure 1. The relationship between the ion exchange ratio and the slit width of hydrogen tetratitanates is summarized in Table 1. The main peaks which correspond to (200) of $H_2Ti_4O_9$ were clearly observed and shifted significantly to lower 2θ angles as the length of $C_nH_{2n+1}NH_2$ increased. These results indicate that the layer structure was maintained during the $C_nH_{2n+1}NH_2$ incorporation and the slit width could expand up to 4.6 nm. The ion exchange ratio was about 20–60 mol %, and the slit widths of obtained samples were about 1.5–2 times the molecular length of $C_nH_{2n+1}NH_2$.

XRD patterns of the samples after TiO_2 incorporation are compared in Figure 2. The main peaks of the samples can be observed and are shifted to lower 2θ angles as the length of $C_nH_{2n+1}NH_2$ increased, indicating that the TiO_2 stacked well and formed a pillar structure in the interlayer.

Representative TG-DTA profiles of the samples after $[Ti(OH)_x(CH_3COO)_y]^{z+}$ incorporation before and after

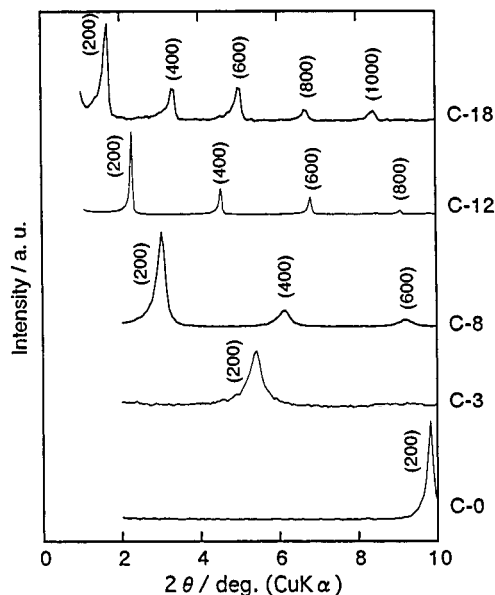


Figure 1. X-ray diffraction patterns after $C_nH_{2n+1}NH_2$ incorporation.

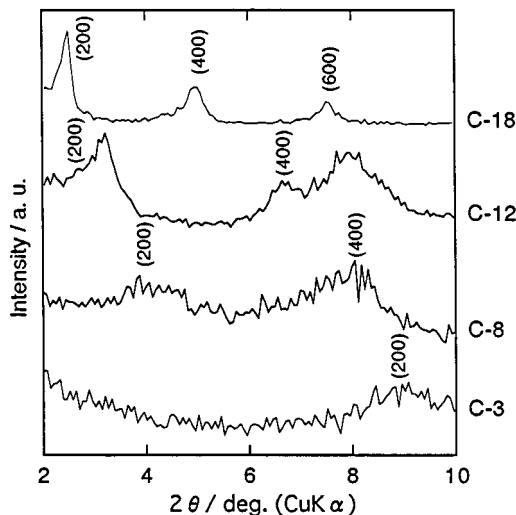


Figure 2. X-ray diffraction patterns after TiO_2 incorporation.

Table 1. Relationship between Ion Exchange Ratio and Interlayer Distance of Hydrogen Titanates

n value in $C_nH_{2n+1}NH_2$	length of $C_nH_{2n+1}NH_2$ (nm)	ion exchange ratio (mol %)	interlayer distance (nm)	bending (deg)
$n = 3$	0.5	45	1.0	0
$n = 8$	1.3	52	2.2	34
$n = 12$	1.9	61	3.1	35
$n = 18$	2.9	24	4.6	38

UV irradiation are shown in Figure 3. A sharp peak and weight loss at 200–400 °C, which corresponds to the combustion of organic species, were observed before UV irradiation, whereas the peak and weight loss for $[Ti(OH)_x(CH_3COO)_y]_zTi_4O_9(C-n)$ disappeared after UV irradiation. In the case of silicates, organic species remaining after incorporation were usually decomposed by calcination.^{1–8,11–13,15–17,39–41} But in this case, UV light irradiation should be used instead of calcination because the host material, $H_2Ti_4O_9$, is thermally unstable above 150 °C.^{18–22,37–38} In Figure 3, it can be seen that organic species were perfectly decomposed by UV light irradiation.

(26) Doeuff, S.; Henry, M.; Sanchez, C.; Livage, J. *J. Non-Cryst. Solids* **1987**, *89*, 206.

(27) Livage, J.; Sanchez, C.; Henry, M.; Doeuff, S. *Solid State Ionics* **1989**, *32/33*, 633.

(28) Kao, C.; Yang, W. *Ceram. Int.* **1996**, *22*, 57.

(29) Yanagisawa, M.; Uchida, S.; Fujishiro, Y.; Sato, T. *J. Mater. Chem.* **1998**, *8*, 2835.

(30) Kitayama, Y.; Kodama, T.; Abe, M.; Simotsuma, H. *J. Porous Mater.* **1998**, *5*, 121.

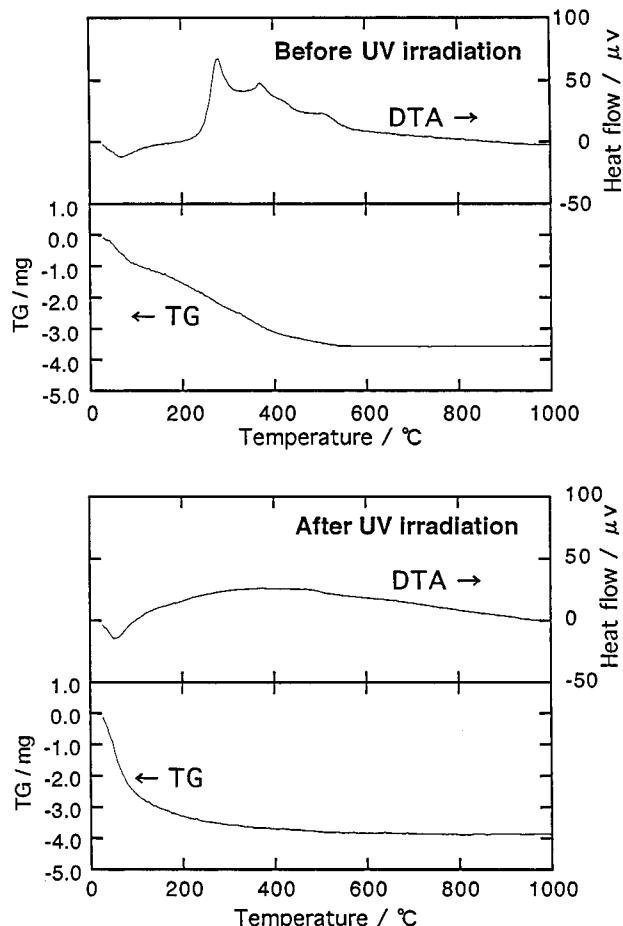


Figure 3. Representative TG and DTA profiles before and after UV irradiation of $\text{H}_2\text{Ti}_4\text{O}_9/\text{TiO}_2(\text{C}-8)$.

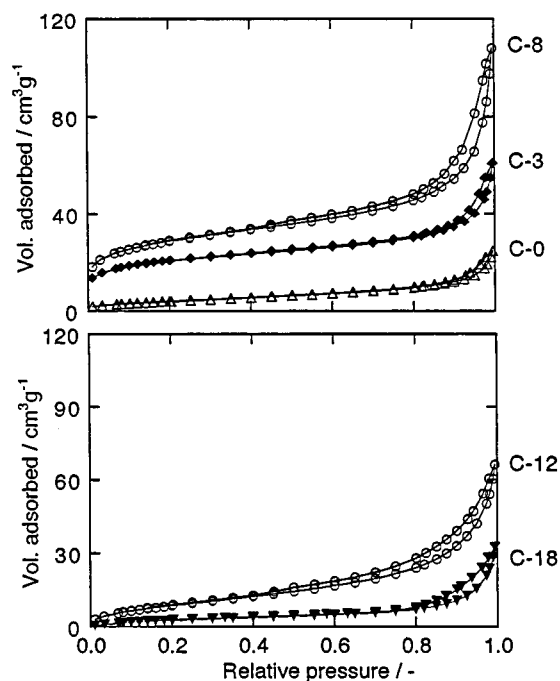


Figure 4. Isotherms of nitrogen adsorption.

Isotherms of nitrogen adsorption at liquid nitrogen temperature for the products are shown in Figure 4. The nitrogen adsorption of C-0 ($\text{H}_2\text{Ti}_4\text{O}_9$) increased and desorption decreased almost normally. The amount of N_2 adsorbed increased at p (relative pressure) = 0.1 and

Table 2. Interlayer Distance and Specific Surface Area of Obtained Samples after Incorporation of TiO_2

	interlayer distance	SSA ($\text{m}^2 \text{g}^{-1}$)
$\text{H}_2\text{Ti}_4\text{O}_9(\text{C}-0)$	0.46	15.3
$\text{H}_2\text{Ti}_4\text{O}_9/\text{TiO}_2(\text{C}-3)$	0.52	72.8
$\text{H}_2\text{Ti}_4\text{O}_9/\text{TiO}_2(\text{C}-8)$	1.5	101.5
$\text{H}_2\text{Ti}_4\text{O}_9/\text{TiO}_2(\text{C}-12)$	2.1	25.0
$\text{H}_2\text{Ti}_4\text{O}_9/\text{TiO}_2(\text{C}-18)$	2.8	9.0

hysteresis appeared in the range of $0.4 < p < 0.99$ as the length of $\text{C}_n\text{H}_{2n+1}\text{NH}_2$ increased up to $n = 8$. The amount of N_2 adsorbed decreased and hysteresis became smaller as n increased. As shown in the IUPAC classification, the isotherm profile of $\text{H}_2\text{Ti}_4\text{O}_9$ was classified as type III, those of $\text{H}_2\text{Ti}_4\text{O}_9/\text{TiO}_2(\text{C}-3)$, $\text{H}_2\text{Ti}_4\text{O}_9/\text{TiO}_2(\text{C}-8)$, and $\text{H}_2\text{Ti}_4\text{O}_9/\text{TiO}_2(\text{C}-12)$ were classified as type IV, and $\text{H}_2\text{Ti}_4\text{O}_9/\text{TiO}_2(\text{C}-18)$ was type V.^{31–32,42} The type V isotherm is rarely observed, indicating that C-18 is a unique material.

Specific surface area (SSA) values determined by 8 points of the Brunauer–Emmett–Teller method and the slit width of $\text{H}_2\text{Ti}_4\text{O}_9/\text{TiO}_2(\text{C}-n)$ are shown in Table 2. The specific surface area increased up to $n = 8$ and decreased although slit width increased as the length of $\text{C}_n\text{H}_{2n+1}\text{NH}_2$ increased. This may be attributed to the large expansion of layer sheets above 50 nm during the intercalation reaction because macropores cannot be characterized by the N_2 adsorption method.⁴²

SEM photographs of $\text{H}_2\text{Ti}_4\text{O}_9/\text{TiO}_2(\text{C}-18)$ are shown in Figure 5. It was clearly observed that slits were expanded significantly by degradation to small fibers. Furthermore, a few nanometer sized slits were also observed. It has been reported that layered compounds can degrade from a layer structure to a gel solution during the incorporation of water and/or long-sized molecules.^{33–36,44} These SEM photographs strongly support the view that the same phenomena occurred during the intercalation treatment. In addition, it is noticeable that the slit width of the nanocomposites is a few nanometers, which is almost equal to that determined by XRD analysis.

Discussion

It has been reported that layered compounds can degrade to gel solution by infinite expansion of layer sheets by the incorporation of a large number of water and/or long-sized molecules.^{33–36,44} Because heptane solution was used in the case of $n \geq 8$, infinite expansion was effectively depressed during the $\text{C}_n\text{H}_{2n+1}\text{NH}_2$ incorporation. On the other hand, the slit widths of C- n were about 1.5–2 times the length of $\text{C}_n\text{H}_{2n+1}\text{NH}_2$, so it was assumed that two $\text{C}_n\text{H}_{2n+1}\text{NH}_2$ molecules connect

(31) (a) Sing, K. S. W.; Everett, D. H.; Haul, R. A. W.; Moscou, L.; Pierotti, R. A.; Rouquerol, T.; Siemienińska, T. *Pure Appl. Chem.* **1985**, *57*, 603. (b) Dollimore, D.; Heal, G. R. *J. Colloid Interface Sci.* **1970**, *33*, 508.

(32) Figueras, F. *Catal. Rev.—Sci. Eng.* **1988**, *30*, 457.

(33) Pinnavaia, T. J.; Landau, S. D.; Tzou, M. S.; Johnson, I. D. *J. Am. Chem. Soc.* **1985**, *107*, 7222.

(34) Aldebert, P.; Baffier, N.; Ledendre, J. J.; Livage, J. *Rev. Chim. Miner.* **1982**, *19*, 485.

(35) Nakato, T.; Furumi, Y.; Okuhara, T. *Chem. Lett.* **1998**, 611.

(36) Inukai, K.; Hotta, Y.; Taniguchi, M.; Tomura, S.; Yamagishi, A. *J. Chem. Soc., Chem. Commun.* **1994**, 959.

(37) Yin, S.; Uchida, S.; Fujishiro, Y.; Aki, M.; Sato, T. *J. Mater. Chem.* **1999**, *9*, 1191.

(38) Marchand, R.; Brohan, L.; Tournoux, M. *Mater. Res. Bull.* **1980**, *15*, 1129.

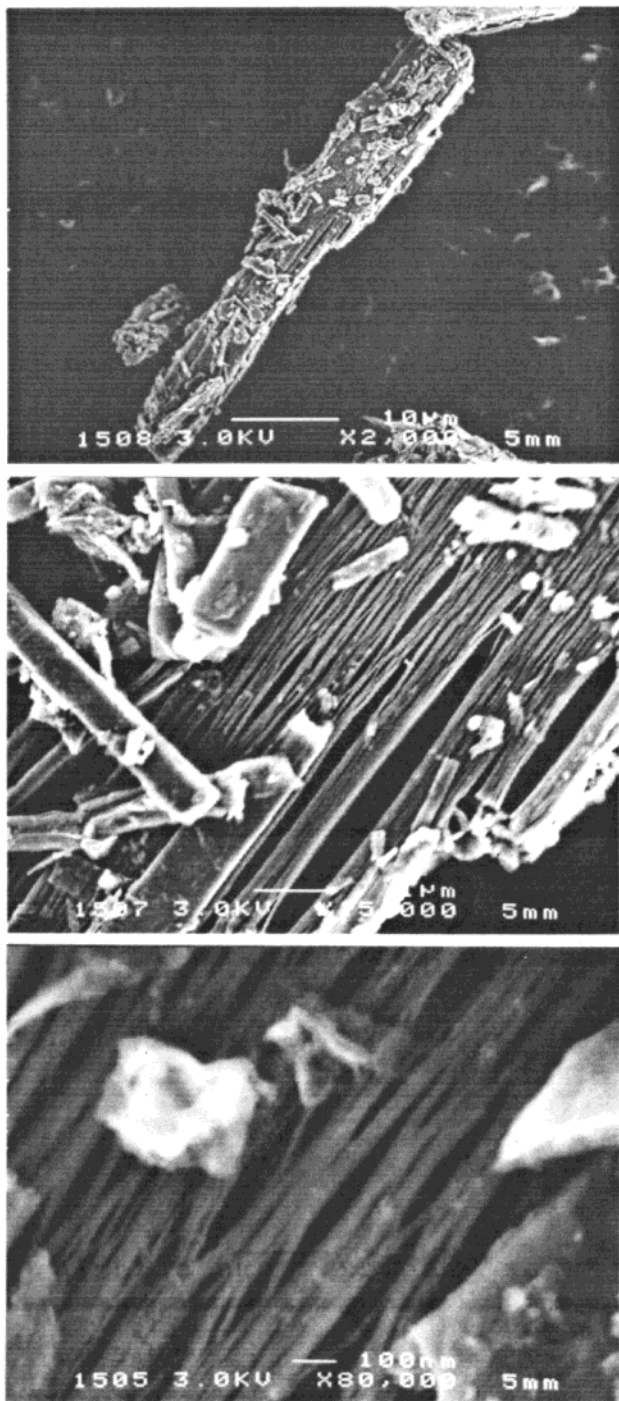


Figure 5. SEM photographs of $H_2Ti_4O_9/TiO_2$ (C-18).

each layer sheet, bending about $0\text{--}40^\circ$ from the a -axis [bending angles were derived by a calculation of $\cos^{-1}\{\text{slit width}/(2 \times \text{the length of } C_nH_{2n+1}NH_2)\}$].

From the XRD patterns after TiO_2 incorporation (Figure 2), the slit width increased as the length of carbon chains increased, although the required time span was 8–20 times longer compared to that for the TiO_2 sol solution.^{21,22,29,43} Because TiO_2 incorporation was carried out in the aqueous solution for a longer time span, infinite expansion would occur by incorporating a large number of water molecules.

From the transition of isotherm profiles and SSA (Figure 4 and Table 2, respectively), it can be concluded that the slit width expanded as the length of C_nH_{2n+1}

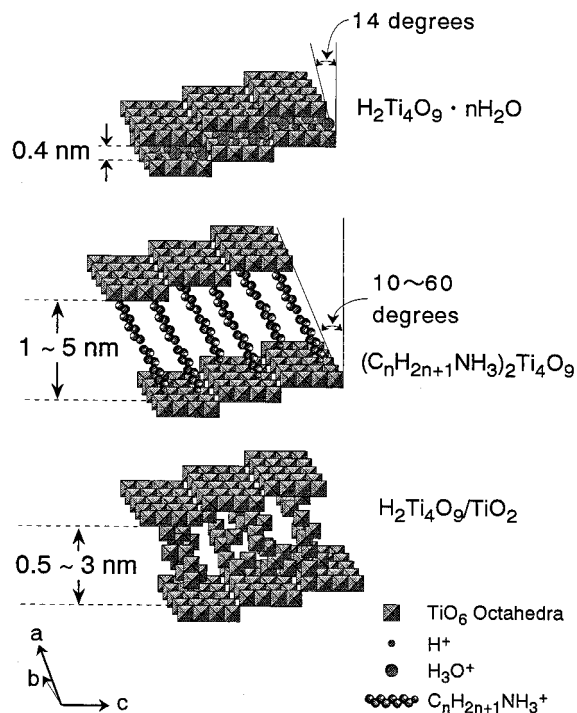


Figure 6. Schematic illustrations of the series of nanocomposites obtained in this study.

NH_2 increased. It is clear that these slits come from the expansion of titanate sheets by the construction of titania pillars via $C_nH_{2n+1}NH_2$ incorporation. Finally, isotherm patterns changed to type V in the case of C-18, indicating that the slit width of C-18 was so large that the interaction of N_2 molecules was weak. From the SEM photograph shown in Figure 5, large expanded slits (slit width was above 50 nm) were observed as well as narrow slits corresponding to the interlayer space (slit width was about a few nanometers as shown in Table 2). The unique isotherm pattern of C-18 exhibits the large and narrow widths of slits produced by the incorporation of TiO_2 and a large number of water molecules via alkylamine. Figure 5 shows the beginning of the infinite expansion of the interlayer and the expanded layer structure of $H_2Ti_4O_9/TiO_2$ (C-18) nanocomposites.

Schematic illustrations of the series of nanocomposites obtained in this study are shown in Figure 6. At first, two $C_nH_{2n+1}NH_2$ molecules connect each layer sheet, bending about $10\text{--}60^\circ$ from the a -axis. In this state, the slit width can be controlled up to 5 nm. Second, TiO_2 was precipitated slowly in the interlayer around the $C_nH_{2n+1}NH_2$ connecting each layer sheet, and slits whose width is controllable from 0.5 to ca. 3 nm along the length of $C_nH_{2n+1}NH_2$ were produced followed by UV irradiation. This can be compared to the model of silicate nanocomposites^{39–41} incorporated by

(39) Choy, J. H.; Park, J. H.; Yoon, J. B. *J. Phys. Chem. B* **1998**, *102*, 5991.

(40) Han, Y. S.; Yamanaka, S.; Choy, J. H. *Appl. Catal., A* **1998**, *174*, 83.

(41) Han, Y. S.; Yamanaka, S.; Choy, J. H. *J. Solid State Chem.* **1998**, *144*, 45.

(42) Kaneko, K. In *Equilibria and Dynamics of Gas Adsorption on Heterogeneous Solid Surfaces*; Rudzinski, W., Steele, W. A., Zgrablich, G., Eds.; Elsevier: New York, 1997; Chapter 13.

(43) Yanagisawa, M.; Uchida, S.; Yin, S.; Sato, T. *Microporous Mesoporous Mater.*, submitted for publication.

using the $\text{SiO}_2\text{-MO}_x$ sol solution. From the SEM observation, the model of most benefit in this study should be that shown in Figure 6.

Conclusion

In this study, the titania-pillared $\text{H}_2\text{Ti}_4\text{O}_9$ was fabricated by the reactions of $\text{H}_2\text{Ti}_4\text{O}_9$ and $\text{C}_n\text{H}_{2n+1}\text{NH}_2$ with a titanyl acylate complex followed by UV irradiation. The slits were produced, and their width could be controlled by changing the length of $\text{C}_n\text{H}_{2n+1}\text{NH}_2$. Furthermore, the slits and the beginning state of infinite

expansion were confirmed by SEM photographs for the first time. From this analysis, we succeeded in constructing the beneficial structure model of the nanocomposites obtained in this study.

Acknowledgment. This work was supported by a Grant-in-Aid for Scientific Research from the Ministry of Education, Science and Culture. The authors thank Mr. Yoshiyuki Nakamura (Ebara Corp.) and Mr. Katsumi Nochi (Mitsubishi Heavy Ind.) for their help in doing the N_2 adsorption-desorption measurements. Special thanks are given to Mr. Aoyagi for the SEM observation.

(44) Sasaki, T.; Watanabe, M.; Hashizume, H.; Yamada, H.; Nakazawa, H. *J. Am. Chem. Soc.* **1996**, *118*, 8329.

CM000335F